

Table 1
Data-collection statistics.

Values in parentheses are for the highest resolution shell (2.8–2.7 Å).	
X-ray source	SPring-8 BL41XU
Space group	$P4_1$ or $P4_3$
Unit-cell parameters (Å, °)	$a = b = 49.96$, $c = 103.20$, $\alpha = \beta = \gamma = 90$
Wavelength (Å)	1.0000
Resolution range (Å)	50.00–2.70 (2.80–2.70)
Total reflections	26984
Unique reflections	6807
$R_{\text{merge}}^{\dagger}$ (%)	4.8 (25.1)
Completeness (%)	97.3 (83.1)
$\langle I/\sigma(I) \rangle$	17.3 (4.5)
Redundancy	4.0 (3.1)
Crystal mosaicity (°)	0.458

$\dagger R_{\text{merge}} = \sum_{hkl} \sum_i |I_i(hkl) - \langle I(hkl) \rangle| / \sum_{hkl} \sum_i I_i(hkl)$, where $I_i(hkl)$ is the i th intensity measurement of reflection hkl and $\langle I(hkl) \rangle$ is its average.

ADSC Quantum 315 CCD detector installed on the BL41XU beamline at SPring-8. The data collection was performed at a wavelength of 1.000 Å over a total range of 180°, with individual frames of 1° and an exposure time of 4 s. The crystal-to-detector distance was 350 mm. The collected images were processed using *HKL2000* (Otwinowski & Minor, 1997).

3. Results and discussion

CHP is an important regulatory factor that maintains the physiologically active conformation of NHE1. In this study, in order to clarify the regulatory mechanism of NHE1 by CHP, we coexpressed CHP2 and its binding domain in NHE1 (amino acids 503–545) in *E. coli* and crystallized the complex. Firstly, we confirmed that the purified complex CHP2–NHE1-peptide was retained as a single peak on gel-filtration chromatography, indicating that the stable complex exists as a monomer ($M_r = 28\,000$) in solution. In addition, using a 4–12% polyacrylamide gradient gel we confirmed that the purity of the complex is suitable for crystallization assay and that the purified sample contained equimolar amounts (1:1 molar ratio) of CHP2 and NHE1-peptide (Fig. 1).

Crystals suitable for X-ray crystallographic analysis were obtained within 2–3 d at 293 K using the sitting-drop vapour-diffusion method (Fig. 2). A previous attempt to collect crystallographic data at beamline BL44B2 (SPring-8) gave a maximum resolution of 3.0 Å owing to the small size of crystals. To obtain higher resolution data, we used the undulator beamline BL41XU. Crystals diffracted to 2.5 Å resolution along the c axis of the crystal, but the data set was only qualitatively useful to 2.7 Å because of anisotropic diffraction.

The tetragonal crystal of CHP2–NHE1-peptide was determined to be $P4_1$ or $P4_3$, with unit-cell parameters $a = b = 49.96$, $c = 103.20$ Å. Assuming the presence of one CHP2–NHE1-peptide complex molecule in the asymmetric unit, the Matthews coefficient V_M was calculated to be $2.5 \text{ \AA}^3 \text{ Da}^{-1}$, indicating a solvent content of approximately 49.5% in the unit cell. These values are within the typical range for protein crystals (Matthews, 1968).

The native data set has 6807 unique reflections, giving a data-set completeness of 97.3% in the resolution range 50.0–2.7 Å, with an $R(I)_{\text{merge}}$ of 4.8% (Table 1). Although CHP2 shows about 36% sequence identity with human CNB (PDB code 1aui; Kissinger *et al.*, 1995), molecular replacement using CNB as a search model with *MOLREP* (Vagin & Teplyakov, 1997) was unsuccessful. Further crystallization refinement and structural analysis by multi-wavelength anomalous dispersion methods using selenomethionine and also taking advantage of the presence of yttrium as an additive are in progress.

We thank the staff at beamlines BL44B2 and BL41XU, SPring-8 for data-collection support and Dr Tianxiang Pang for initial participation in this study. This work was supported by grant Nano-001 for Research on Advanced Medical Technology from the Ministry of Health, Labour and Welfare of Japan and Grant-in-Aid for Priority Areas 13142210 for Scientific Research from the Ministry of Education, Science and Culture of Japan. YBA was supported by a Japan Society for the Promotion of Science (JSPS) Postdoctoral Fellowship.

References

- Barroso, M. R., Bernd, K. K., DeWitt, N. D., Chang, A., Mills, K. & Sztul, E. S. (1996). *J. Biol. Chem.* **271**, 10183–10187.
- Bertrand, B., Wakabayashi, S., Ikeda, T., Pouyssegur, J. & Shigekawa, M. (1994). *J. Biol. Chem.* **269**, 13703–13709.
- Counillon, L. & Pouyssegur, J. (2000). *J. Biol. Chem.* **275**, 1–4.
- Kissinger, C. R., Parge, H. E., Knighton, D. R., Lewis, C. T., Pelletier, L. A., Tempczyk, A., Kalish, V. J., Tucker, K. D., Showalter, R. E., Moomaw, E. W., Gastinel, L. N., Habuka, N., Chen, X., Maldonado, F., Barker, J. E., Bacquet, R. & Villafranca, J. E. (1995). *Nature (London)*, **378**, 641–644.
- Lin, X. & Barber, D. L. (1996). *Proc. Natl Acad. Sci. USA*, **93**, 12631–12636.
- Lin, X., Sikkink, R. A., Rusnak, F. & Barber, D. L. (1999). *J. Biol. Chem.* **274**, 36125–36131.
- Matsumoto, M., Miyake, Y., Nagita, M., Inoue, H., Shitakubo, D., Takemoto, K., Ohtsuka, C., Murakami, H., Nakamura, N. & Kanazawa, H. (2001). *J. Biochem.* **130**, 217–225.
- Matthews, B. W. (1968). *J. Mol. Biol.* **33**, 491–497.
- Nakamura, N., Miyake, Y., Matsushita, M., Tanaka, S., Inoue, H. & Kanazawa, H. (2002). *J. Biochem.* **132**, 483–491.
- Orlowski, J. & Grinstein, S. (2004). *Pflugers Arch.* **447**, 549–565.
- Otwinowski, Z. & Minor, W. (1997). *Methods Enzymol.* **276**, 307–326.
- Pang, T., Hisamitsu, T., Mori, H., Shigekawa, M. & Wakabayashi, S. (2004). *Biochemistry*, **43**, 3628–3636.
- Pang, T., Su, X., Wakabayashi, S. & Shigekawa, M. (2001). *J. Biol. Chem.* **276**, 17367–17372.
- Pang, T., Wakabayashi, S. & Shigekawa, M. (2002). *J. Biol. Chem.* **277**, 43771–43777.
- Putney, L. K., Denker, S. P. & Barber, D. L. (2002). *Annu. Rev. Pharmacol. Toxicol.* **42**, 527–552.
- Timm, S., Titus, B., Bernd, K. & Barroso, M. (1999). *Mol. Biol. Cell*, **10**, 3473–3488.
- Vagin, A. A. & Teplyakov, A. (1997). *J. Appl. Cryst.* **30**, 1022–1025.
- Wakabayashi, S., Bertrand, B., Ikeda, T., Pouyssegur, J. & Shigekawa, M. (1994). *J. Biol. Chem.* **269**, 13710–13715.
- Wakabayashi, S., Shigekawa, M. & Pouyssegur, J. (1997). *Physiol. Rev.* **77**, 51–74.

Conventional enhanced K-edge angiography utilizing cerium x-ray generator

Eiichi Sato^a, Akira Yamadera^b, Toshio Ichimaru^b, Etsuro Tanaka^c, Hidezo Mori^d, Toshiaki Kawai^e, Takashi Inoue^f, Akira Ogawa^f, Shigehiro Sato^g, Kazuyoshi Takayama^h
and Hideaki Idoⁱ

^a Department of Physics, Iwate Medical University, 3-16-1 Honchodori, Morioka 020-0015, Japan

^b Department of Radiological Technology, School of Health Sciences, Hirosaki University, 66-1 Honcho, Hirosaki 036-8564, Japan

^c Department of Nutritional Science, Faculty of Applied Bio-science, Tokyo University of Agriculture, 1-1-1 Sakuragaoka, Setagaya-ku 156-8502, Japan

^d Department of Cardiac Physiology, National Cardiovascular Center Research Institute, 5-7-1 Fujishirodai, Suita, Osaka 565-8565, Japan

^e Electron Tube Division #2, Hamamatsu Photonics K. K., 314-5 Shimokanzo, Toyooka Village, Iwata-gun 438-0193, Japan

^f Department of Neurosurgery, School of Medicine, Iwate Medical University, 19-1 Uchimaru, Morioka 020-8505, Japan

^g Department of Microbiology, School of Medicine, Iwate Medical University, 19-1 Uchimaru, Morioka 020-8505, Japan

^h Shock Wave Research Center, Institute of Fluid Science, Tohoku University, 2-1-1 Katahira, Sendai 980-8577, Japan

ⁱ Department of Applied Physics and Informatics, Faculty of Engineering, Tohoku Gakuin University, 1-13-1 Chuo, Tagajo 985-8537, Japan

Abstract

The cerium-target x-ray tube is useful in order to perform cone-beam K-edge angiography because K α rays from the cerium target are absorbed effectively by iodine-based contrast media. The maximum tube voltage and current were 65 kV and 0.40 mA, respectively, and the focal-spot sizes were approximately 1×1 mm. Sharp cerium K α lines were left using a barium sulfate filter, and the x-ray

intensity was $16.8 \mu\text{Gy/s}$ at 1.0 m from the source with a tube voltage of 60 kV and a current of 0.40 mA. Angiography was performed using iodine-based microspheres $15 \mu\text{m}$ in diameter. In angiography of non-living animals, we observed fine blood vessels of $100 \mu\text{m}$ or less.

1. Introduction

Synchrotrons generate monochromatic parallel x-ray beams using single crystals. These beams with photon energies of approximately 35 keV have been employed to perform enhanced K-edge angiography,¹⁻³ since the beams are absorbed effectively by iodine-based contrast media.

In order to perform high-speed medical radiography, although several different flash x-ray generators⁴⁻⁹ utilizing cold-cathode tubes have been developed, plasma flash x-ray generators¹⁰⁻¹³ are useful to produce quasi-monochromatic x rays without using a K-edge filter. Therefore, we have performed a demonstration of cone-beam K-edge angiography¹⁴ utilizing a cerium plasma generator, since K-series characteristic x rays from the cerium target are absorbed effectively by iodine. Recently, we have developed a steady-state x-ray generator utilizing a cerium-target tube, and have demonstrated enhanced K-edge angiography utilizing a barium sulfate filter.¹⁵ In this research, $K\alpha$ lines (34.6 keV) were left by absorbing $K\beta$ lines (39.2 keV).

In the present research, we describe a preliminary study on cone-beam K-edge angiography achieved with cerium $K\alpha$ rays using a barium sulfate filter.

2. Generator

Figure 1 shows the block diagram of the x-ray generator, which consists of a main controller, a cerium-target x-ray tube unit with a Cockcroft-Walton circuit and an insulation transformer, and a personal computer. The tube voltage, the current, and the exposure time can be controlled by both the controller and the computer. The main circuit for producing x rays is illustrated in Fig. 2, and employs the Cockcroft-Walton circuit in order to decrease the dimensions of the tube unit. In the x-ray tube, the negative high-voltage is applied to the cathode electrode, and the anode (target) is connected to the tube unit case (ground potential) to cool the anode and the target effectively. The filament heating current is supplied by an AC power supply in the controller in conjunction with an insulation transformer. In this experiment, the tube voltage applied was from 45 to 65 kV, and the tube current was regulated to within 0.40 mA (maximum current) by the filament temperature. The exposure time is controlled in order to obtain optimum x-ray intensity. Monochromatic $K\alpha$ lines were left using a 5-mm-thick barium sulfate filter in which barium sulfate powder was mixed with polymethyl methacrylate (PMMA) resin, since both the bremsstrahlung and the $K\beta$ rays were absorbed effectively by the filter. In designing the filter, the surface density of the barium sulfate powder is important, since the x rays are absorbed effectively by the powder as compared with the PMMA resin. In this case, the density was approximately 10 mg/cm^2 .

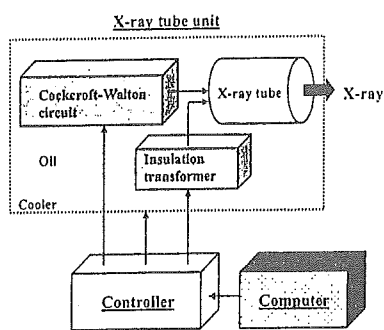


Fig. 1: Block diagram of compact x-ray generator with cerium-target tube.

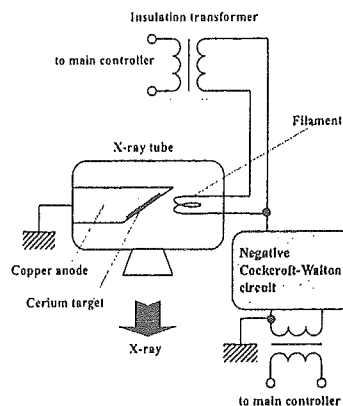


Fig. 2: Main circuit of x-ray generator.

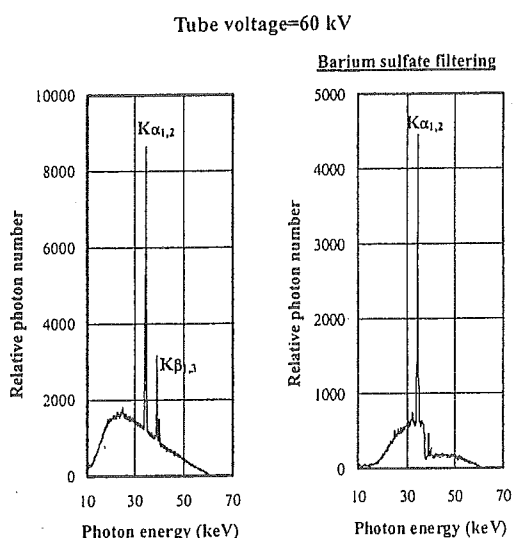


Fig. 3: X-ray spectra measured using germanium detector and filter.

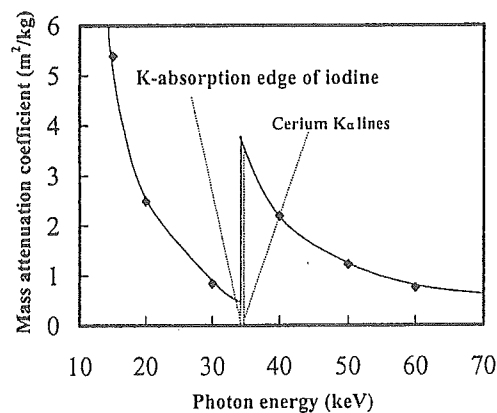


Fig. 4: Mass attenuation coefficients of iodine, and average photon energy of cerium K α lines.

3. Characteristics

The x-ray intensity rate was measured by a Victoreen 660 ionization chamber at 1.0 m from the x-ray source. At a constant tube current of 0.40 mA, the x-ray intensity increased when the tube voltage was increased. In this measurement, the intensity with a tube voltage of 60 kV and a current of 0.40 mA was 16.8 $\mu\text{Gy/s}$ with errors of less than 0.2%.

In order to measure images of the x-ray source, we employed a pinhole camera with a hole diameter of 50 μm in conjunction with a Computed Radiography (CR) system¹⁶ with a sampling pitch of 87.5 μm . When the tube voltage was increased, spot dimensions increased slightly and had values of

approximately 1×1 mm.

In order to measure x-ray spectra, we employed a germanium detector (GLP-10180/07-P, Ortec Inc.) (Fig. 3). When the tube voltage was increased, the $K\alpha$ intensity substantially increased, and both the maximum photon energy and the intensities of bremsstrahlung x rays increased.

4. Angiography

Figure 4 shows the mass attenuation coefficients of iodine at the selected energies; the coefficient curve is discontinuous at the iodine K-edge. The average photon energy of the cerium $K\alpha$ lines is shown just above the iodine K-edge. Cerium is a rare earth element and has a high reactivity; however, the average photon energies of $K\alpha$ is 34.6 keV, and iodine contrast mediums with a K-absorption edge of 33.2 keV absorb the lines easily. Therefore, blood vessels were observed with high contrasts.

The angiography was performed using the CR system (Konica Regius 150), iodine microspheres of $15 \mu\text{m}$ in diameter, and the filter. The distance (between the x-ray source and the imaging plate) was 1.5 m, and the tube voltage was 60 kV. Figure 5 shows angiograms of an extracted dog heart. Because the size of the dog heart is almost the same as human heart, human coronary arteries can be observed.

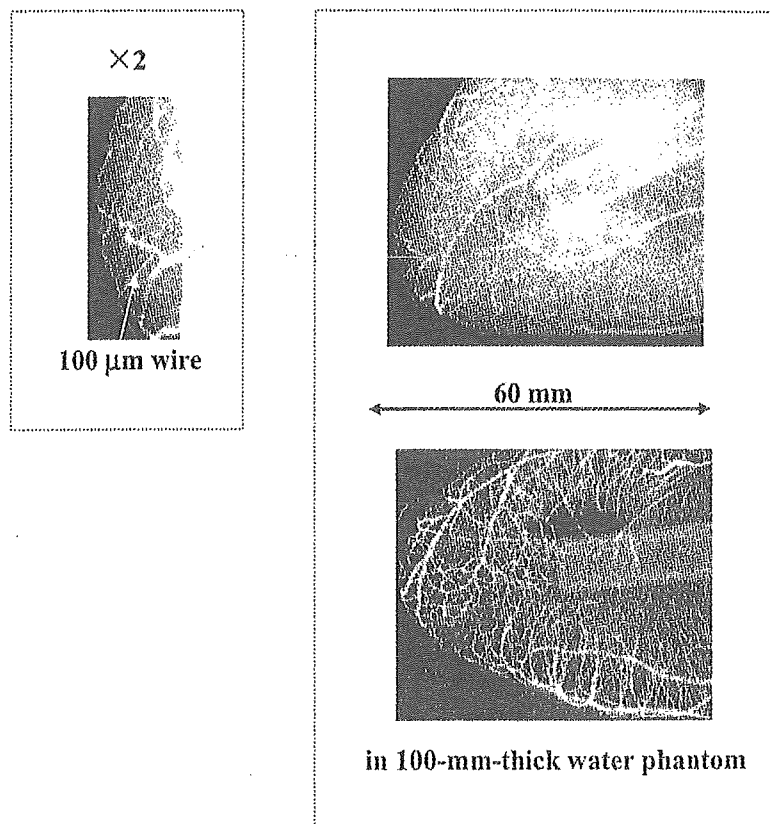


Fig. 5: Angiogram of extracted dog heart using iodine microspheres.

5. Discussion and Conclusions

In summary, we developed a new x-ray generator with a cerium-target tube and succeeded in producing cerium $K\alpha$ lines, which can be absorbed easily by iodine-based contrast media. Both the characteristic and bremsstrahlung x-ray intensities increased with increases in the tube voltage, and $K\beta$ lines were absorbed effectively by the barium sulfate filter.

In this preliminary experiment, although the maximum tube voltage and current were 65 kV and 0.40 mA, respectively, the voltage and current could be increased. Subsequently, the generator produced maximum number of $K\alpha$ photons was approximately 3×10^7 photons/cm²·s at 1.0 m from the source, and the photon count rate can be increased easily by improving the target.

Acknowledgment

This work was supported by Grants-in-Aid for Scientific Research (13470154, 13877114, and 16591222) and Advanced Medical Scientific Research from MECSST, Health and Labor Sciences Research Grants (RAMT-nano-001, RHGTEFB-genome-005 and RHGTEFB-saisei-003), Grants from Keiryō Research Foundation, The Promotion and Mutual Aid Corporation for Private Schools of Japan, Japan Science and Technology Agency (JST), and New Energy and Industrial Technology Development Organization (NEDO, Industrial Technology Research Grant Program in '03).

References

1. A. C. Thompson, H. D. Zeman, G. S. Brown, J. Morrison, P. Reiser, V. Padmanabahn, L. Ong, S. Green, J. Giacomini, H. Gordon and E. Rubenstein, "First operation of the medical research facility at the NSLS for coronary angiography," *Rev. Sci. Instrum.*, **63**, 625-628, 1992.
2. H. Mori, K. Hyodo, E. Tanaka, M. U. Mohammed, A. Yamakawa, Y. Shinozaki, H. Nakazawa, Y. Tanaka, T. Sekka, Y. Iwata, S. Honda, K. Umetani, H. Ueki, T. Yokoyama, K. Tanioka, M. Kubota, H. Hosaka, N. Ishizawa and M. Ando, "Small-vessel radiography in situ with monochromatic synchrotron radiation," *Radiology*, **201**, 173-177, 1996.
3. K. Hyodo, M. Ando, Y. Oku, S. Yamamoto, T. Takeda, Y. Itai, S. Ohtsuka, Y. Sugishita and J. Tada, "Development of a two-dimensional imaging system for clinical applications of intravenous coronary angiography using intense synchrotron radiation produced by a multipole wiggler," *J. Synchrotron Rad.*, **5**, 1123-1126, 1998.
4. E. Sato, H. Isobe and F. Hoshino, "High intensity flash x-ray apparatus for biomedical radiography," *Rev. Sci. Instrum.*, **57**, 1399-1408, 1986.
5. E. Sato, S. Kimura, S. Kawasaki, H. Isobe, K. Takahashi, Y. Tamakawa and T. Yanagisawa, "Repetitive flash x-ray generator utilizing a simple diode with a new type of energy-selective function," *Rev. Sci. Instrum.*, **61**, 2343-2348, 1990.
6. A. Shikoda, E. Sato, M. Sagae, T. Oizumi, Y. Tamakawa and T. Yanagisawa, "Repetitive flash x-ray

- generator having a high-durability diode driven by a two-cable-type line pulser," *Rev. Sci. Instrum.*, **65**, 850-856, 1994.
7. E. Sato, K. Takahashi, M. Sagae, S. Kimura, T. Oizumi, Y. Hayasi, Y. Tamakawa and T. Yanagisawa, "Sub-kilohertz flash x-ray generator utilizing a glass-enclosed cold-cathode triode," *Med. & Biol. Eng. & Comput.*, **32**, 289-294, 1994.
 8. E. Sato, M. Sagae, E. Tanaka, Y. Hayasi, R. Germer, H. Mori, T. Kawai, T. Ichimaru, S. Sato, K. Takayama and H. Ido, "Quasi-monochromatic flash x-ray generator utilizing a disk-cathode molybdenum tube," *Jpn. J. Appl. Phys.*, **43**, 7324-7328, 2004.
 9. E. Sato, E. Tanaka, H. Mori, T. Kawai, T. Ichimaru, S. Sato, K. Takayama and H. Ido, "Compact monochromatic flash x-ray generator utilizing a disk-cathode molybdenum tube," *Med. Phys.*, **32**, 49-54, 2005.
 10. E. Sato, Y. Hayasi, R. Germer, E. Tanaka, H. Mori, T. Kawai, H. Obara, T. Ichimaru, K. Takayama and H. Ido, "Irradiation of intense characteristic x-rays from weakly ionized linear molybdenum plasma," *Jpn. J. Med. Phys.*, **23**, 123-131, 2003.
 11. E. Sato, Y. Hayasi, R. Germer, E. Tanaka, H. Mori, T. Kawai, T. Ichimaru, K. Takayama and H. Ido, "Quasi-monochromatic flash x-ray generator utilizing weakly ionized linear copper plasma," *Rev. Sci. Instrum.*, **74**, 5236-5240, 2003.
 12. E. Sato, R. Germer, Y. Hayasi, Y. Koorikawa, K. Murakami, E. Tanaka, H. Mori, T. Kawai, T. Ichimaru, F. Obata, K. Takahashi, S. Sato, K. Takayama and H. Ido, "Weakly ionized plasma flash x-ray generator and its distinctive characteristics," *SPIE*, **5196**, 383-392, 2003.
 13. E. Sato, Y. Hayasi, R. Germer, E. Tanaka, H. Mori, T. Kawai, T. Ichimaru, S. Sato, K. Takayama and H. Ido, "Sharp characteristic x-ray irradiation from weakly ionized linear plasma," *J. Electron Spectrosc. Related Phenom.*, **137-140**, 713-720, 2004.
 14. E. Sato, R. Germer, Y. Hayasi, K. Murakami, Y. Koorikawa, E. Tanaka, H. Mori, T. Kawai, T. Ichimaru, F. Obata, K. Takahashi, S. Sato, K. Takayama and H. Ido, "Weakly ionized cerium plasma radiography," *SPIE*, **5210**, 12-21, 2003.
 15. E. Sato, E. Tanaka, H. Mori, T. Kawai, T. Ichimaru, S. Sato, K. Takayama and H. Ido, "Demonstration of enhanced K-edge angiography using a cerium target x-ray generator," *Med. Phys.*, **31**, 3017-3021, 2004.
 16. E. Sato, K. Sato and Y. Tamakawa, "Film-less computed radiography system for high-speed imaging," *Ann. Rep. Iwate Med. Univ. Sch. Lib. Arts and Sci.*, **35**, 13-23, 2000.

**Preliminary experiment for producing higher harmonic x rays
utilizing copper plasma triode**

Eiichi Sato^a, Etsuro Tanaka^b, Hidezo Mori^c, Toshiaki Kawai^d, Takashi Inoue^e, Akira Ogawa^e,
Shigehiro Sato^f, Kazuyoshi Takayama^g and Hideaki Ido^h

^a Department of Physics, Iwate Medical University, 3-16-1 Honchodori, Morioka 020-0015,
Japan

^b Department of Nutritional Science, Faculty of Applied Bio-science, Tokyo University of
Agriculture, 1-1-1 Sakuragaoka, Setagaya-ku 156-8502, Japan

^c Department of Cardiac Physiology, National Cardiovascular Center Research Institute, 5-7-1
Fujishirodai, Suita, Osaka 565-8565, Japan

^d Electron Tube Division #2, Hamamatsu Photonics K. K., 314-5 Shimokanzo, Toyooka
Village, Iwata-gun 438-0193, Japan

^e Department of Neurosurgery, School of Medicine, Iwate Medical University,
19-1 Uchimaru, Morioka 020-8505, Japan

^f Department of Microbiology, School of Medicine, Iwate Medical University, 19-1 Uchimaru,
Morioka 020-8505, Japan

^g Shock Wave Research Center, Institute of Fluid Science, Tohoku University, 2-1-1 Katahira,
Sendai 980-8577, Japan

^h Department of Applied Physics and Informatics, Faculty of Engineering, Tohoku Gakuin
University, 1-13-1 Chuo, Tagajo 985-8537, Japan

Abstract

In the plasma flash x-ray generator, a 200 nF condenser is charged up to 50 kV by a power supply, and flash x rays are produced by the discharging. The x-ray tube is a demountable triode with a trigger electrode, and the turbomolecular pump evacuates air from the tube with a pressure of approximately 1 mPa. Target evaporation leads to the formation of weakly ionized linear plasma, consisting of copper ions and electrons, around the fine target, and intense $K\alpha$ lines are left using a 10- μ m-thick nickel filter. At a charging voltage of 50 kV, the maximum tube voltage was almost equal to the charging voltage of the main condenser, and the peak current was about 15 kA. The K-series characteristic x

rays were clean and intense, and higher harmonic x rays were observed. The x-ray pulse widths were approximately 700 ns, and the time-integrated x-ray intensity had a value of approximately 20 $\mu\text{C}/\text{kg}$ at 1.0 m from the x-ray source with a charging voltage of 50 kV.

1. Introduction

Recently, soft x-ray lasers have been produced by a gas-discharge capillary,¹⁻⁴ and the laser pulse energy substantially increased in proportion to the capillary length. However, it is difficult to increase the laser photon energy to 10 keV or beyond. Because there are no x-ray resonators in the high-photon-energy region, new methods for increasing coherence will be desired in the future. To perform high-speed soft radiography, several different flash x-ray generators⁵⁻¹⁰ have been developed corresponding to specific objectives. Subsequently, we have developed a compact flash x-ray generator utilizing a disk-cathode demountable diode,^{11,12} and have performed a preliminary experiment for producing clean characteristic x rays utilizing angle dependence of bremsstrahlung x rays.

With recent advances in high-voltage pulse technology, several different plasma flash x-ray generators have been developed corresponding to specific radiographic objectives, and a major goal in our research is the development of an intense and sharp monochromatic x-ray generator that can impact applications with biomedical radiography.

In this paper, we describe a plasma flash x-ray generator¹³⁻¹⁵ utilizing a rod-target radiation tube, used to perform a preliminary experiment for generating intense and clean K-series characteristic x rays and their higher harmonic x rays by forming a linear copper plasma cloud around a fine target.

2. Generator

Figure 1 shows a block diagram of the high-intensity plasma flash x-ray generator. This generator consists of the following essential components: a high-voltage power supply, a high-voltage condenser with a capacity of approximately 200 nF, a turbomolecular pump, a krytron pulse generator as a trigger device, and a flash x-ray tube. The high-voltage main condenser is charged to 50 kV by the power supply, and electric charges in the condenser are discharged to the tube after triggering the cathode electrode with the trigger device. The plasma flash x rays are then produced.

The x-ray tube is a demountable cold-cathode triode that is connected to the turbomolecular pump with a pressure of approximately 1 mPa. This tube consists of the following major parts: a hollow cylindrical carbon cathode with a bore diameter of 10.0 mm, a brass focusing electrode, a trigger electrode made from copper wire, a stainless steel vacuum chamber, a nylon insulator, a polyethylene terephthalate (Mylar) x-ray window 0.25 mm in thickness, and a rod-shaped copper target 3.0 mm in diameter with a tip angle of 60°. The distance between the target and cathode electrodes is

approximately 20 mm, and the trigger electrode is set in the cathode electrode. As electron beams from the cathode electrode are roughly converged to the target by the focusing electrode, evaporation leads to the formation of a weakly ionized linear plasma, consisting of copper ions and electrons, around the fine target.

In the linear plasma, bremsstrahlung photons with energies higher than the K-absorption edge are effectively absorbed and are converted into fluorescent x rays (Fig. 2). The plasma then transmits the fluorescent rays easily, and bremsstrahlung rays with energies lower than the K-edge are also absorbed by the plasma. In addition, because bremsstrahlung rays are not emitted in the opposite direction to that of electron acceleration, intense characteristic x rays are generated from the plasma-axial direction.

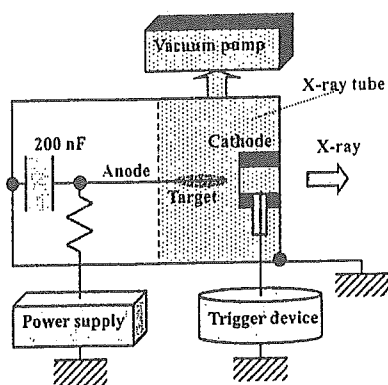


Fig. 1: Block diagram including electric circuit of plasma flash x-ray generator.

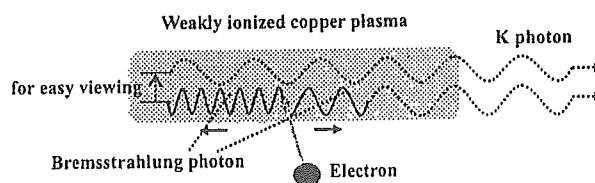


Fig. 2: K-photon irradiation from plasma.

3. Characteristics

Tube voltage and current were measured by a high-voltage divider with an input impedance of 1 G Ω and a current transformer, respectively. At a charging voltage of 50 kV, the maximum tube voltage was almost equal to the charging voltage of the main condenser, and the maximum tube current was approximately 15 kA.

X-ray output pulse was detected by a combination of a plastic scintillator and a photomultiplier using a 10- μ m-thick nickel filter. The x-ray pulse height substantially increased with corresponding increases in the charging voltage. The x-ray pulse widths were about 700 ns, and the time-integrated x-ray intensity per pulse measured by a thermoluminescence dosimeter (Kyokko TLD Reader 1500 utilizing MSO-S elements without energy compensation) had a value of about 20 μ C/kg at 1.0 m from the x-ray source with a charging voltage of 50 kV.

X-ray spectra from the plasma source were measured by a transmission-type spectrometer with a lithium fluoride curved crystal 0.5 mm in thickness. The spectra were taken by a computed radiography (CR) system¹⁶ (Konica Regius 150) with a wide dynamic range, using the filter, and

relative x-ray intensity was calculated from Dicom digital data. Figure 3 shows measured spectra from the copper target with a charging voltage of 50 kV. In fact, we observed clean K lines such as lasers, and $K\alpha$ lines were left by absorbing $K\beta$ lines using the filter. The characteristic x-ray intensity substantially increased with corresponding increases in the charging voltage, and higher harmonic x rays were observed.

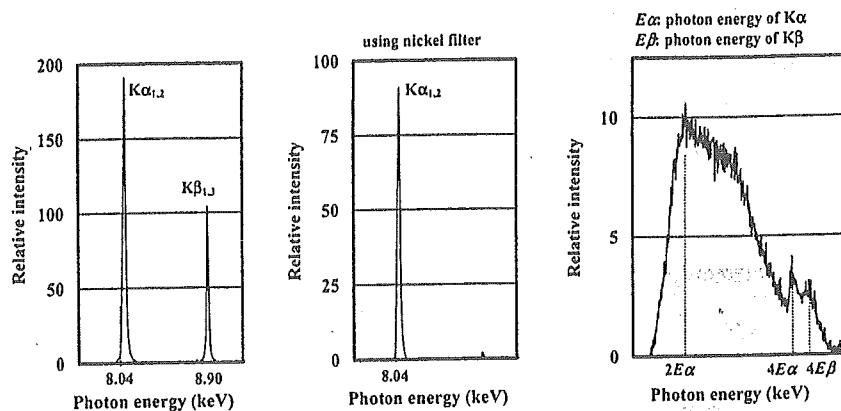


Fig. 3: X-ray spectra from weakly ionized copper plasma at indicated conditions.

4. Radiography

The plasma radiography was performed by the CR system using the filter. The charging voltage and the distance between the x-ray source and imaging plate were 50 kV and 1.2 m, respectively.

Firstly, an image of plastic bullets falling into a polypropylene beaker from a plastic test tube is shown in Fig. 4. Because the x-ray duration was about $1 \mu\text{s}$, the stop-motion image of bullets could be obtained. Figure 5 shows an angiogram of a rabbit ear; iodine-based microspheres of $15 \mu\text{m}$ in diameter were used, and fine blood vessels of about $50 \mu\text{m}$ were visible.

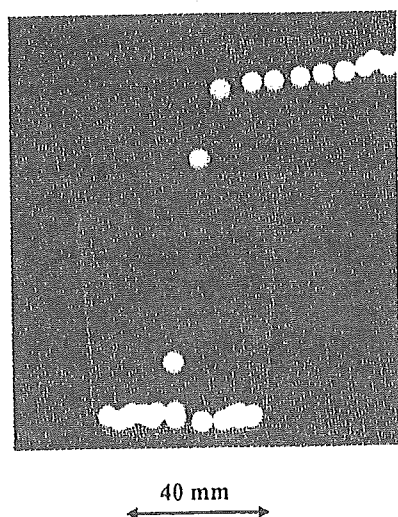


Fig. 4: Radiogram of water falling into polypropylene beaker from plastic test tube.

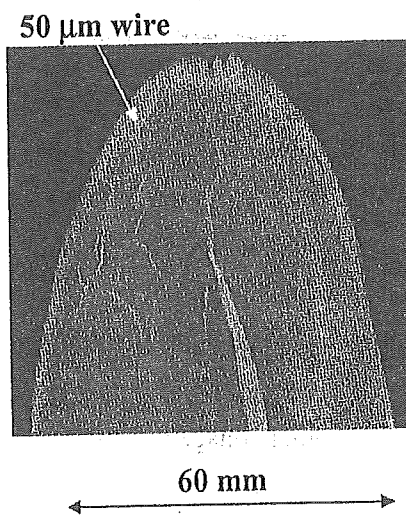


Fig. 5: Angiograms of rabbit ear.

5. Discussion and Conclusions

Concerning the spectrum measurement, we obtained fairly intense and clean K lines from a weakly ionized linear plasma x-ray source, and $K\alpha$ lines were left by absorbing $K\beta$ lines using the nickel filter. In particular, the higher harmonic x rays were produced from the plasma. Assuming that the harmonic rays are produced by the x-ray resonance (Fig. 6), the estimated spectra are shown in Fig. 7. In cases where a copper target is employed, fractional harmonic x rays are absorbed by an x-ray window and air.

In this research, we obtained sufficient characteristic x-ray intensity per pulse for CR radiography, and the generator produced number of characteristic $K\alpha$ photons was approximately 5×10^7 photons/cm² at 1.0 m per pulse. In addition, since the photon energy of characteristic x rays can be controlled by changing the target elements, various quasi-monochromatic high-speed radiographies, such as high-contrast angiography and mammography, will be possible.

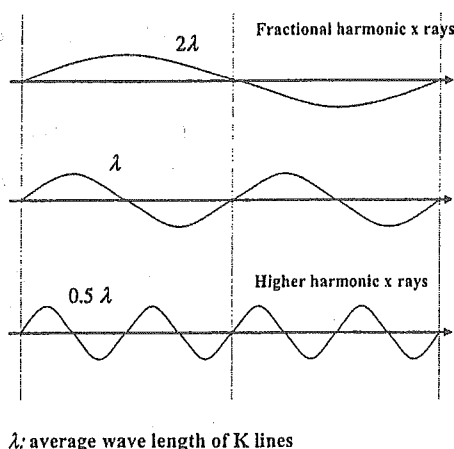


Fig. 6: X-ray resonance without using resonator.

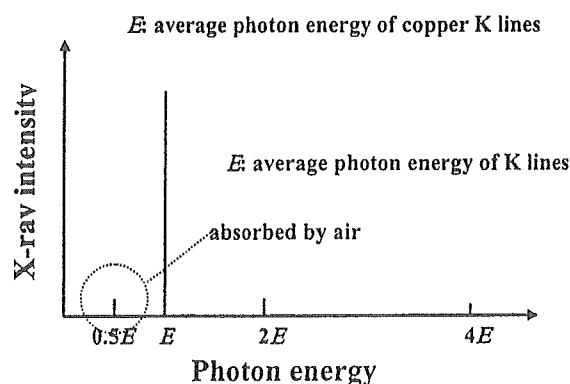


Fig. 7: Estimated x-ray spectra under resonance.

Acknowledgment

This work was supported by Grants-in-Aid for Scientific Research (13470154, 13877114, and 16591222) and Advanced Medical Scientific Research from MECSST, Health and Labor Sciences Research Grants (RAMT-nano-001, RHGTEFB-genome-005 and RHGTEFB-saisei-003), Grants from Keiryō Research Foundation, The Promotion and Mutual Aid Corporation for Private Schools of Japan, Japan Science and Technology Agency (JST), and New Energy and Industrial Technology Development Organization (NEDO, Industrial Technology Research Grant Program in '03).

References

1. J.J. Rocca, V. Shlyaptsev, F.G. Tomasel, O.D. Cortazar, D. Hartshorn and J.L.A. Chilla, "Demonstration of a discharge pumped table-top soft x-ray laser," *Proc. Phys. Lev. Lett.*, **73**,

2192-2195, 1994.

2. J.J. Rocca, D.P. Clark, J.L.A. Chilla and V.N. Shlyaptsev, "Energy Extration and achievement of the saturation limit in a discharge-pumped table-top soft x-ray amplifier," *Phys. Lev. Lett.*, **77**, 1476-1479, 1996.
3. C.D. Macchietto, B.R. Benware and J.J. Rocca, "Generation of millijoule-level soft-x-ray laser pulses at a 4-Hz repetition rate in a highly saturated tabletop capillary discharge amplifier," *Opt. Lett.*, **24**, 1115-1117, 1999.
4. J.J.G. Rocca, J.L.A. Chilla, S. Sakadzic, A. Rahman, J. Filevich, E. Jankowska, E.C. Hammarsten, B.M. Luther, H.C. Kapteyn, M. Murnane and V.N. Shlyapsev, "Advances in capillary discharge soft x-ray laser research," *Proc. SPIE*, **4505**, 1-6 2001.
5. A. Mattsson, "Some characteristics of a 600 kV flash x-ray tube," *Physica Scripta*, **5**, 99-102, 1972.
6. R. Germer, "X-ray flash techniques," *J. Phys. E: Sci. Instrum.*, **12**, 336-350, 1979.
7. E. Sato, S. Kimura, S. Kawasaki, H. Isobe, K. Takahashi, Y. Tamakawa and T. Yanagisawa, "Repetitive flash x-ray generator utilizing a simple diode with a new type of energy-selective function," *Rev. Sci. Instrum.*, **61**, 2343-2348, 1990.
8. A. Shikoda, E. Sato, M. Sagae, T. Oizumi, Y. Tamakawa and T. Yanagisawa, "Repetitive flash x-ray generator having a high-durability diode driven by a two-cable-type line pulser," *Rev. Sci. Instrum.*, **65**, 850-856, 1994.
9. E. Sato, K. Takahashi, M. Sagae, S. Kimura, T. Oizumi, Y. Hayasi, Y. Tamakawa and T. Yanagisawa, "Sub-kilohertz flash x-ray generator utilizing a glass-enclosed cold-cathode triode," *Med. & Biol. Eng. & Comput.*, **32**, 289-294, 1994.
10. K. Takahashi, E. Sato, M. Sagae, T. Oizumi, Y. Tamakawa and T. Yanagisawa, "Fundamental study on a long-duration flash x-ray generator with a surface-discharge triode," *Jpn. J. Appl. Phys.*, **33**, 4146-4151, 1994.
11. E. Sato, M. Sagae, E. Tanaka, Y. Hayasi, R. Germer, H. Mori, T. Kawai, T. Ichimaru, S. Sato, K. Takayama and H. Ido, "Quasi-monochromatic flash x-ray generator utilizing a disk-cathode molybdenum tube," *Jpn. J. Appl. Phys.*, **43**, 7324-7328, 2004.
12. E. Sato, E. Tanaka, H. Mori, T. Kawai, T. Ichimaru, S. Sato, K. Takayama and H. Ido, "Compact monochromatic flash x-ray generator utilizing a disk-cathode molybdenum tube," *Med. Phys.*, **32**, 49-54, 2005.
13. E. Sato, Y. Hayasi, R. Germer, E. Tanaka, H. Mori, T. Kawai, H. Obara, T. Ichimaru, K. Takayama and H. Ido, "Irradiation of intense characteristic x-rays from weakly ionized linear molybdenum plasma," *Jpn. J. Med. Phys.*, **23**, 123-131, 2003.
14. E. Sato, R. Germer, Y. Hayasi, Y. Koorikawa, K. Murakami, E. Tanaka, H. Mori, T. Kawai, T. Ichimaru, F. Obata, K. Takahashi, S. Sato, K. Takayama and H. Ido, "Weakly ionized plasma flash x-ray generator and its distinctive characteristics," *SPIE*, **5196**, 383-392, 2003.
15. E. Sato, Y. Hayasi, R. Germer, E. Tanaka, H. Mori, T. Kawai, T. Ichimaru, S. Sato, K. Takayama

and H. Ido, "Sharp characteristic x-ray irradiation from weakly ionized linear plasma," *J. Electron Spectrosc. Related Phenom.*, **137-140**, 713-720, 2004.

16. E. Sato, K. Sato and Y. Tamakawa, "Film-less computed radiography system for high-speed Imaging," *Ann. Rep. Iwate Med. Univ. Sch. Lib. Arts and Sci.*, **35**, 13-23, 2000.

Quasi-monochromatic fine polycapillary imaging utilizing computed radiography system

— X-ray lens for biomedicine —

Toshio ICHIMARU*¹, Eiichi SATO*², Etsuro TANAKA*³
Hidezo MORI*⁴, Toshiaki KAWAI*⁵, Sigehiro SATO*⁶
and Kazuyoshi TAKAYAMA*⁷

(Received October 31, 2004 ; Accepted January 13, 2005)

Abstract : A fundamental study on quasi-monochromatic radiography using a polycapillary plate and a copper-target x-ray tube is described. The tube voltage was regulated from 12 to 22 kV, and the tube current was regulated within 3.0 mA by the filament temperature. The exposure time was controlled in order to obtain optimum x-ray intensity, and the maximum focal spot dimensions were approximately 2.0×1.5 mm. The polycapillary plate was J5022-16 (Hamamatsu Photonics Inc.), and the plate thickness was 1.0 mm. The outer, effective, and hole diameters were 33 mm, 27 mm, and $10 \mu\text{m}$, respectively. Quasi-monochromatic x rays were produced using a $10\text{-}\mu\text{m}$ -thick copper filter with a tube voltage of 17 kV, and these rays were formed into quasi-parallel beams by the polycapillary. The radiogram was taken using a computed radiography system utilizing imaging plates. The spatial resolution hardly varied according to increases in the distance between the spatial resolution-test chart and imaging plate using a polycapillary. We could observe a $50 \mu\text{m}$ tungsten wire, and fine blood vessels of approximately $100 \mu\text{m}$ were visible in angiography.

Key words : quasi-parallel radiography, quasi-monochromatic xrays, characteristic xrays, x-ray lens, polycapillary plate

1. INTRODUCTION

Monochromatic parallel x-ray beams are typically produced by a synchrotron in conjunction with single crystals and have been applied in high contrast

micro-angiography¹⁾ and x-ray phase imaging.²⁻⁴⁾

In order to produce quasi-monochromatic x rays without using the synchrotron, we developed a transmission type molybdenum x-ray tube.⁵⁾ Subsequently, flash x-ray tubes are employed to

*¹ Department of Radiological Technology, School of Health Sciences, Hirosaki University, 66-1 Hon-cho, Hirosaki-shi, Aomori-ken 036-8564, Japan.
E-mail: ichimaru@cc.hirosaki-u.ac.jp

*² Department of Physics, Iwate Medical University, 3-16-1 Hon-cho-dori, Morioka-shi, Iwate-ken 020-0015, Japan.

*³ Department of Nutritional Science, Faculty of Applied Bio-science, Tokyo University of Agriculture, 1-1-1 Sakuragaoka, Setagaya-ku, Tokyo 156-8502, Japan.

*⁴ Department of Cardiac Physiology, National Cardiovascular Center Research Institute, 5-7-1 Fujishiro-dai, Suita-shi, Osaka 565-8565, Japan.

*⁵ Electron Tube Division, Hamamatsu Photonics K. K., 314-5 Shimokan-za, Toyooka village, Iwata-gun, Shizuoka-ken, 438-0193, Japan.

*⁶ Department of Microbiology, School of Medicine, Iwate Medical University, 19-1 Uchimarui, Morioka-shi, Iwate-ken 020-8505, Japan.

*⁷ Shock Wave Research Center, Institute of Fluid Science, Tohoku University, 2-1-1 Katahira, Aoba-ku, Sendai-shi, Miyagi-ken 980-8577, Japan.

primarily perform high-speed radiographies with biomedical applications. In particular, plasma flash x-ray tubes are very useful to produce intense and sharp characteristic xrays⁶⁻¹¹⁾ such as lasers.

With recent advances in x-ray optics, several different x-ray lenses^{12,13)} have been developed, and a polycapillary plate^{5, 8,14)} has been shown to be useful to realize a low-priced x-ray system and to perform quasi-parallel radiography. Therefore, we performed polycapillary imaging using a tungsten-target x-ray tube and an x-ray film because the film is conventional and is useful to obtain a high image resolution.

In biomedical radiography, because both the brightness and the contrast of radiograms can be controlled by a Computed Radiography (CR) system¹⁵⁾ utilizing imaging plates, the CR system is useful to perform quasi-monochromatic polycapillary imaging, regardless of whether the image resolution falls.

In this article, we describe a quasi-monochromatic parallel radiography system utilizing a fine polycapillary plate with a hole diameter of 10 μm , a CR system, and a copper-target radiation tube in order to create a conventional x-ray system to be used instead of the synchrotron.

2. EXPERIMENTAL SETUP

Figure 1 shows the circuit diagram of the x-ray generator, which consists of a negative high-voltage power supply, a filament (hot cathode) power supply,

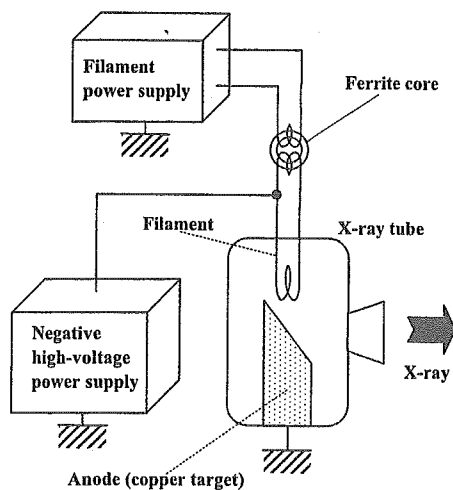


Fig. 1. Circuit diagram of the x-ray generator.

and a copper-target x-ray tube. The negative high-voltage is applied to the cathode electrode, and the anode (target) is connected to the ground. In this experiment, the tube voltage was regulated from 12 to 22 kV, and the tube current was regulated by the filament temperature and ranged from 1.0 to 3.0 mA. The exposure time was controlled in order to obtain optimum x-ray intensity.

The experimental setup for performing quasi-parallel radiography is shown in Fig. 2. Quasi-monochromatic x rays are produced using a 10- μm -thick copper filter, and these rays are formed into quasi-parallel beams by a polycapillary plate (Fig. 3). The polycapillary is J5022-16 (Hamamatsu Photonics Inc.), and the thickness and the hole diameter of the polycapillary are 1.0 mm and 10 μm , respectively. Radiography

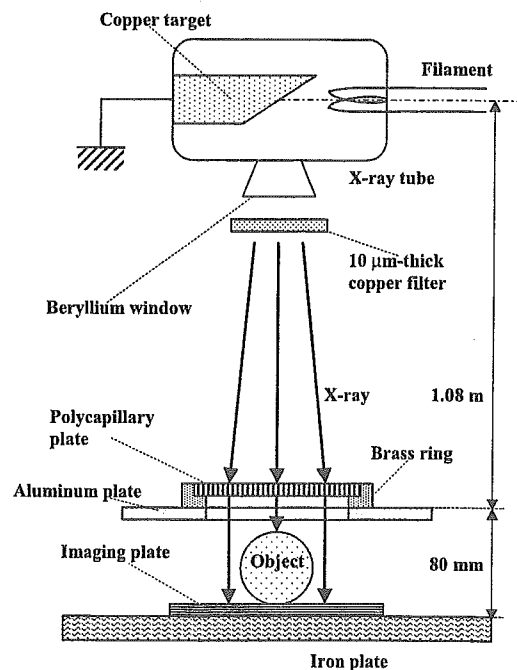
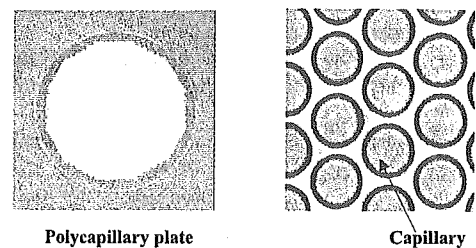


Fig. 2. Experimental setup for quasi-parallel radiography utilizing a polycapillary plate and a CR system.



Polycapillary plate

Capillary

Fig. 3. Polycapillary plate.

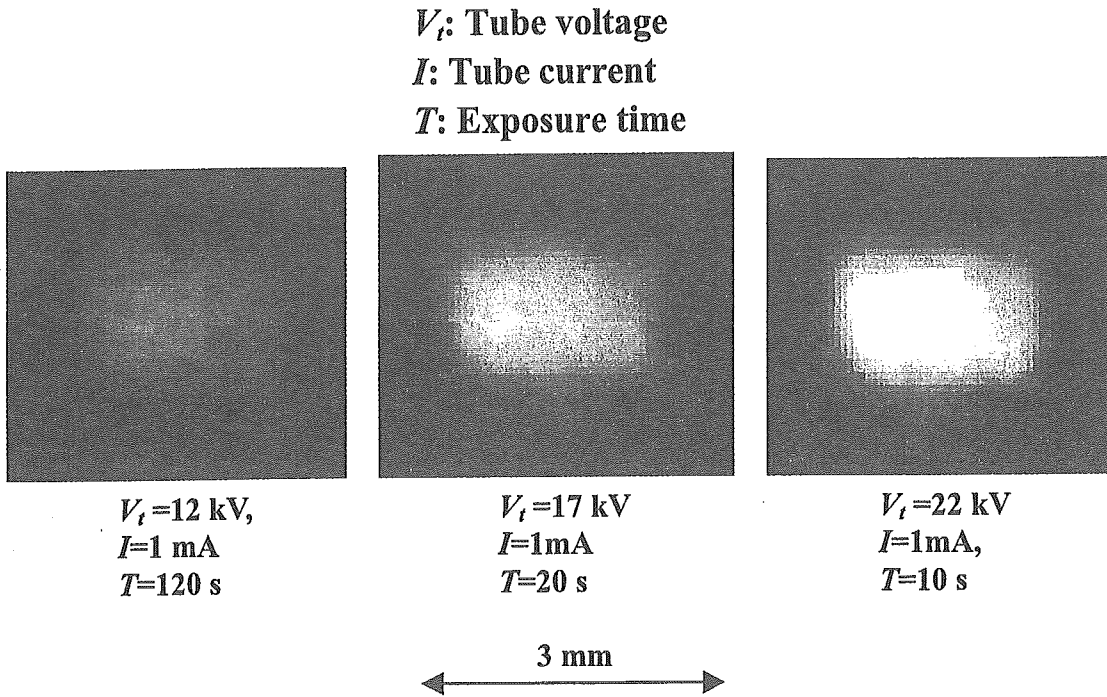


Fig. 4. Images of the x-ray source measured by a 50- μ m-diameter pinhole with changes in the tube voltage.

was performed by a CR system (Konica Regius 150) utilizing imaging plates, and the distance between the x-ray source and the polycapillary was 1.08 m.

3. CHARACTERISTICS

3.1 Focal Spot

In order to measure images of the x-ray source, we employed a pinhole camera with a hole diameter of 50 μ m (Fig. 4). When the tube voltage was increased, the spot intensity increased, and spot dimensions increased slightly and had values of approximately 2.0×1.5 mm.

3.2 X-ray Spectra

X-ray spectra from the copper-target tube were measured by a transmission-type spectrometer with a lithium fluoride curved crystal 0.5 mm in thickness. The spectra were taken by the CR system with a wide dynamic range, and relative x-ray intensity was calculated from DICOM (Digital Imaging and Communications in Medicine) digital data. Figure 5 shows measured spectra from the copper target. When the tube voltage was increased, the bremsstrahlung x-ray intensity increased, and the characteristic x-ray intensity of $K\alpha$ and $K\beta$ lines also increased. Following insertion of the copper filter, the bremsstrahlung x

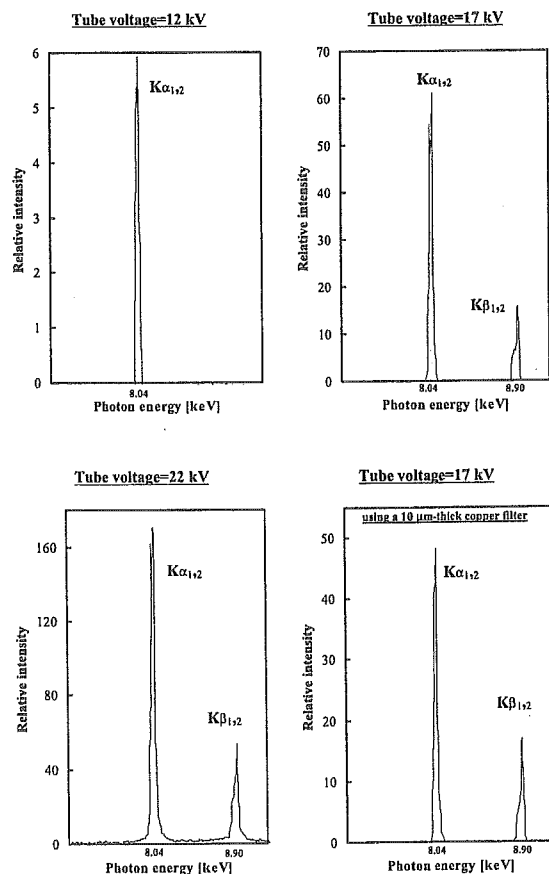


Fig. 5. Measured x-ray spectra according to changes in the tube voltage using a 10- μ m-thick copper filter.

rays with energies higher than the K-absorption edge were absorbed effectively.

4. RADIOGRAPHY

The quasi-monochromatic radiography was performed with a tube voltage of 17 kV using the filter. Figure 6 shows radiography for imaging a polycapillary plate, and the radiograms of the polycapillary are shown in Fig. 7. The center of the black spot in the polycapillary radiogram was mainly imaged by direct transmission beams through capillary holes. As shown in this figure, the spot dimensions increased slightly according to decreases in the polymethyl methacrylate (PMMA) spacer height.

Figure 8 shows the polycapillary radiography for imaging a test chart, and the polycapillary was set

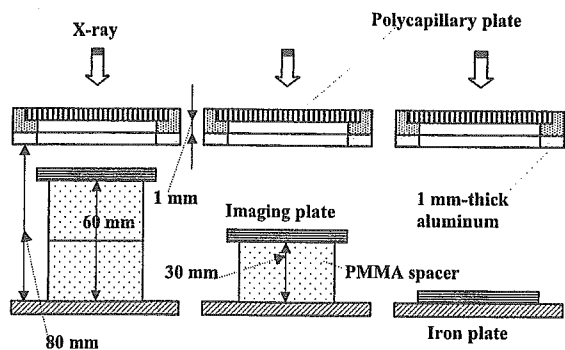


Fig. 6. Radiography for imaging a polycapillary plate according to changes in the distance between the polycapillary and imaging plates.

on the brass ring. In this radiography, when the spacer height was increased, the image resolution hardly varied, and the image dimensions decreased slightly (Fig. 9). Enlarged radiograms of the test chart (166 μm lead lines) are shown in Figs. 10 and 11. When the polycapillary was employed, the image contrast of lines increased, but the resolution hardly varied. With increases in the brass spacer height, the image resolution hardly varied, and the dimensions again decreased slightly (Figs. 12 and 13). When the polycapillary was employed in conjunction with the brass spacer, the contrast again increased.

Figures 14 and 15 show radiography and the radiogram of tungsten wires on a PMMA spacer, respectively. Although the image contrast increased with increases in the wire diameter, a 50 μm -diameter wire could be observed. An angiography of a rabbit heart (coronary artery) is shown in Fig. 16; iodine-based microspheres of 15 μm diameter were used, and fine blood vessels of about 50 μm were visible (Fig. 17).

5. DISCUSSION

In this research, we performed quasi-parallel radiography achieved with a polycapillary plate in conjunction with quasi-monochromatic x rays, and obtained slightly higher image resolutions as compared with those obtained without using the plate.

H_p : PMMA spacer height

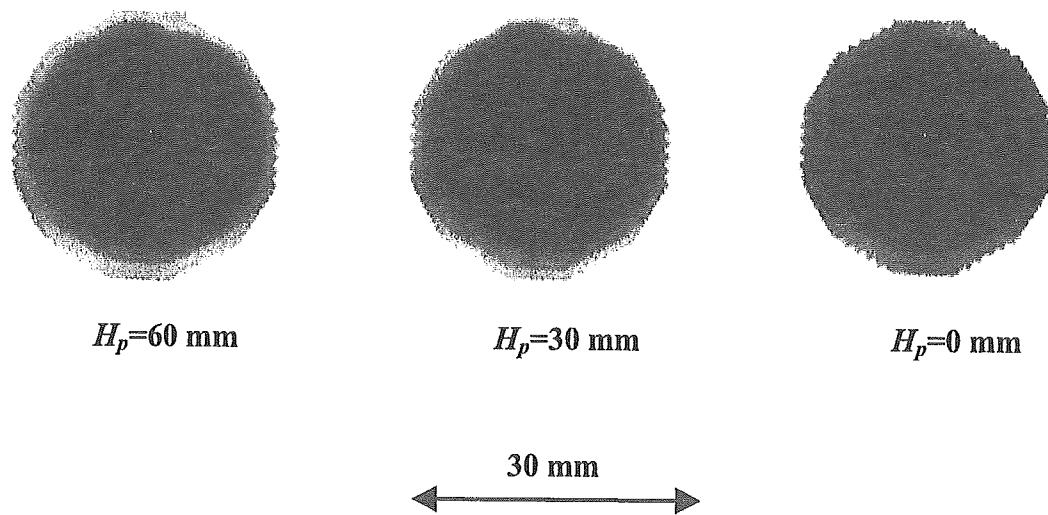


Fig. 7. Radiograms of a polycapillary plate according to changes in the PMMA height.

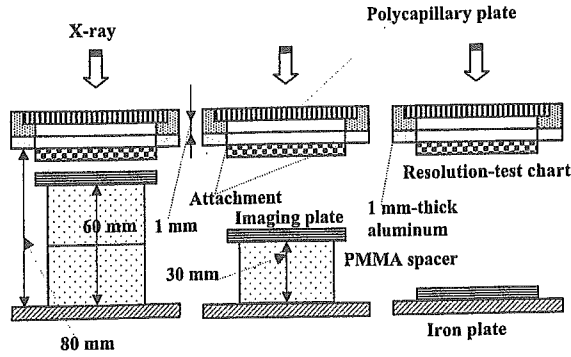


Fig. 8. Radiography for imaging a test chart using a polycapillary plate according to the PMMA height.

If we assume that the capillaries are completely straight, the image resolution of the polycapillary is primarily determined by the diameter of the capillary hole and the thickness, and is improved with decreases in the capillary diameter and increases in the thickness. In cases where the CR system is employed, although the resolution of the CR system is primarily determined by the minimum sampling pitch of $87.5 \mu\text{m}$, we could observe $50 \mu\text{m}$ tungsten wires easily.

The photon energies of the characteristic x rays

H_p : PMMA spacer height

100 μm

125 μm

166 μm

$H_p=60 \text{ mm}$

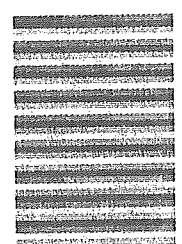
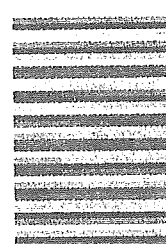
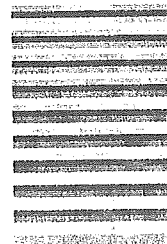
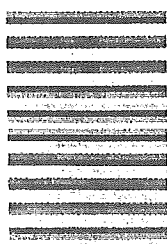
$H_p=30 \text{ mm}$

$H_p=0 \text{ mm}$

Fig. 9. Radiograms of a test chart using a polycapillary plate according to the PMMA height.

166 μm lead lines

166 μm lead lines



$H_p=60 \text{ mm}$

$H_p=30 \text{ mm}$

$H_p=0 \text{ mm}$

$H_p=60 \text{ mm}$

$H_p=30 \text{ mm}$

$H_p=0 \text{ mm}$

H_p : PMMA spacer height

H_p : PMMA spacer height

Fig. 10. Enlarged radiograms of a test chart using a polycapillary plate according to the PMMA height.

Fig. 11. Enlarged radiograms of a test chart without using a polycapillary plate according to the PMMA height.

are determined by the target element, and the capillary thickness should be increased according to increases in the photon energy because the transmission intensity through capillary glass increases. Subsequently, in order to increase the parallelity for phase imaging, single crystals should be employed after passing through the polycapillary.

Because it is possible to increase the irradiation field by increasing the distance between the x-ray source and the polycapillary, this system can be applied to image a wide variety of objects in various fields, including medical radiography.

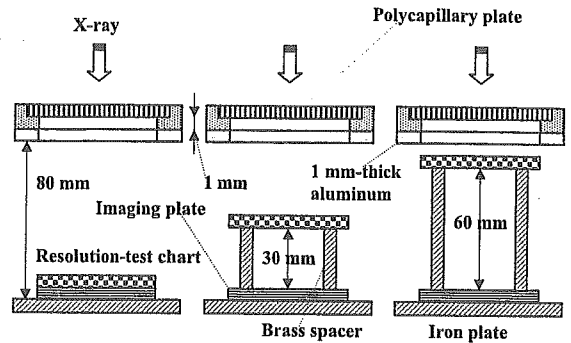


Fig. 12. Radiography for imaging a test chart using a polycapillary plate according to the brass spacer height.

H_b : Brass spacer height

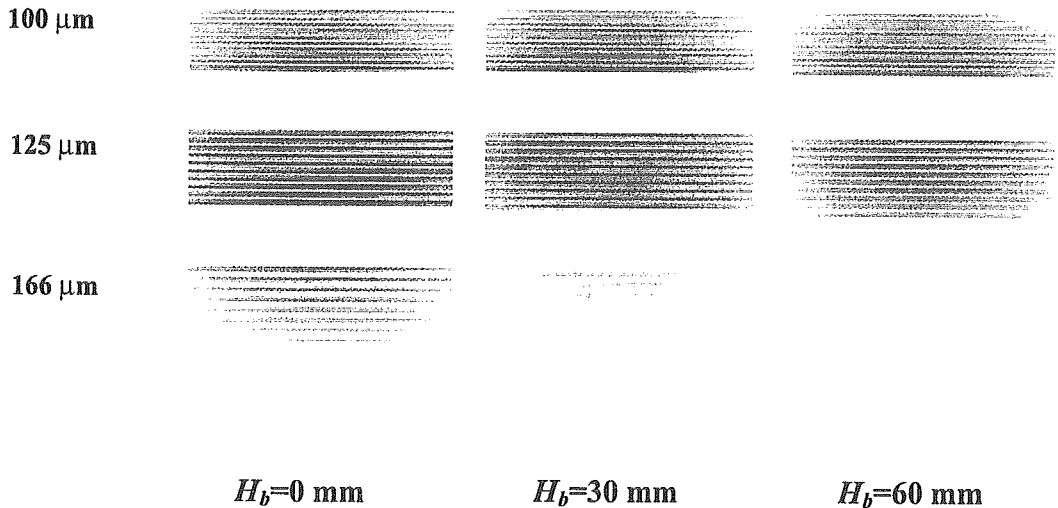


Fig. 13. Radiograms of a test chart using the polycapillary according to the brass spacer height.

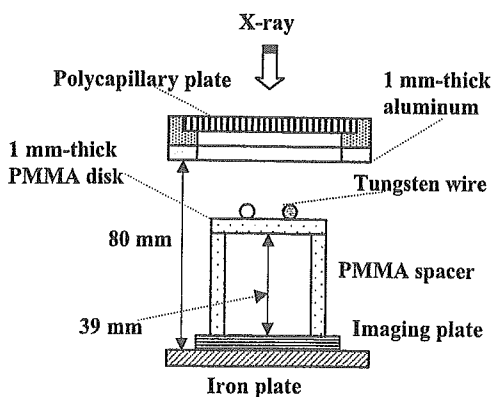


Fig. 14. Radiography for imaging tungsten wires using the polycapillary.

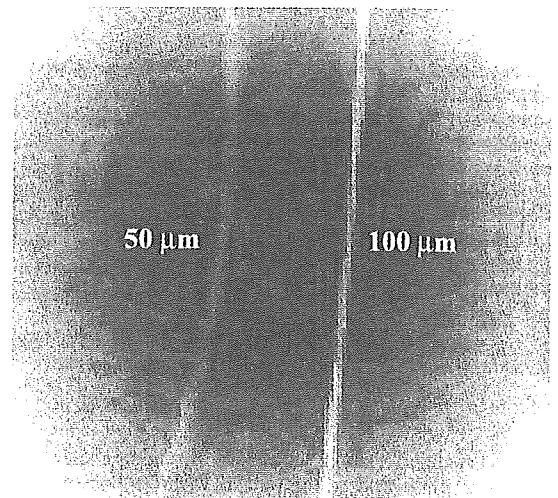


Fig. 15. Radiograms of tungsten wires on a PMMA spacer.